8-15-2003

Repairing the Sickle Cell Mutation. II. Effect of Psoralen Linker Length on Specificity of Formation and Yield of Third Strand-Directed Photoproducts with the Mutant Target Sequence

Olga Amosova
Princeton University

Steven Broitman
West Chester University, sbroitman@wcupa.edu

Jacques R. Fresco
Princeton University

Recommended Citation
Amosova, O., Broitman, S., & Fresco, J. R. (2003). Repairing the Sickle Cell Mutation. II. Effect of Psoralen Linker Length on Specificity of Formation and Yield of Third Strand-Directed Photoproducts with the Mutant Target Sequence. *Nucleic Acids Research, 31*(16), 4673-4681. http://dx.doi.org/10.1093/nar/gkg659

Nucleic Acids Research, 2003, Vol. 31, No. 16 ***4673–4681***
DOI: 10.1093/nar/gkg659

Repairing the Sickle Cell mutation. II. Effect of psoralen linker length on specificity of formation and yield of third strand-directed photoproducts with the mutant target sequence

Olga Amosova[1], Steven L. Broitman[1,2] and Jacques R. Fresco[1,*]

[1]Department of Molecular Biology, Princeton University, Princeton, NJ 08544, USA and [2]Department of Biology, West Chester University, West Chester, PA 19383, USA

Received June 10, 2003; Revised and Accepted June 18, 2003

ABSTRACT

Three identical deoxyoligonucleotide third strands with a 3′-terminal psoralen moiety attached by linkers that differ in length (*N* = 16, 6 and 4 atoms) and structure were examined for their ability to form triplex-directed psoralen photoproducts with both the mutant T residue of the Sickle Cell β-globin gene and the comparable wild-type sequence in linear duplex targets. Specificity and yield of UVA (365 nm) and visible (419 nm) light-induced photoadducts were studied. The total photoproduct yield varies with the linker and includes both monoadducts and crosslinks at various available pyrimidine sites. The specificity of photoadduct formation at the desired mutant T residue site was greatly improved by shortening the psoralen linker. In particular, using the N-4 linker, psoralen interaction with the residues of the non-coding duplex strand was essentially eliminated, while modification of the Sickle Cell mutant T residue was maximized. At the same time, the proportion of crosslink formation at the mutant T residue upon UV irradiation was much greater for the N-4 linker. The photoproducts formed with the wild-type target were fully consistent with its single base pair difference. The third strand with the N-4 linker was also shown to bind to a super-coiled plasmid containing the Sickle Cell mutation site, giving photoproduct yields comparable with those observed in the linear mutant target.

INTRODUCTION

Nucleic acid third strand binding provides a logical approach to the targeting of specific gene sequences for the purpose of transcriptional regulation (1–3), DNA modification (4) and site-directed mutagenesis (5–7). Unique sequence triplex-forming oligonucleotides are able to recognize and associate with duplex DNA targets with great specificity (8,9) provided that purine-rich·pyrimidine-rich tracks of appropriate length are available (10). This specificity of triplex formation (11), combined with the capacity to synthesize third strands with covalently linked reactive reagents, can lead to powerful tools for causing site-specific chemical damage or modification at selected gene sequences. Recently, this approach was used successfully to deliver DNA-modifying reagents adjacent to specific sequences in purified chromosomal DNA (12,13) and nuclei (14), and to target chromosomes *in vivo* (15), opening the way to potential therapeutic applications.

Third strand-directed psoralen modification, for example, has been used to target specific gene sequences *in vivo*, and thereby to trigger repair mechanisms to replace the damaged nucleotides (16–18). Thus, psoralen adduct formation generally leads to base changes at the adduct site, particularly to T·A→A·T conversion (6,19). As an A·T→T·A transversion mutation is responsible for Sickle Cell Anemia, psoralen modification of the Sickle Cell mutant T residue holds promise for triggering the correction of that mutation *in vivo* (20). Towards that end, it is very important to limit the psoralen modification to just the mutant residue, and so to minimize its potential reactivity at any nearby pyrimidine residues within reach of the psoralen moiety borne by the third strand. The Sickle Cell mutation site is located immediately upstream of a 6-bp homopurine·homopyrimidine duplex segment adjacent to a longer pyrimidine-rich·purine-rich segment that can potentially serve as a target for third strand binding (Fig. 1a). This target deviates significantly from the stereochemical regularity most amenable to third strand binding, and required a specially designed third strand in order to achieve triplex-directed psoralen photoaddition at the mutant T residue in a linear model system (20).

In this report, we describe the effect of psoralen linker length and structure on the specificity, efficiency and type of photoadducts formed at the mutation site of Sickle Cell Anemia in a linear duplex target. Photoadduct formation at the comparable site in the wild-type β-globin gene (Fig. 1b) is also examined.

MATERIALS AND METHODS

Deoxyoligonucleotides

These were synthesized by automated phosphoramidite chemistry, purified by denaturing PAGE and recovered from

*To whom correspondence should be addressed. Tel: +1 609 258 3927; Fax: +1 609 258 2759; Email: jrfresco@princeton.edu

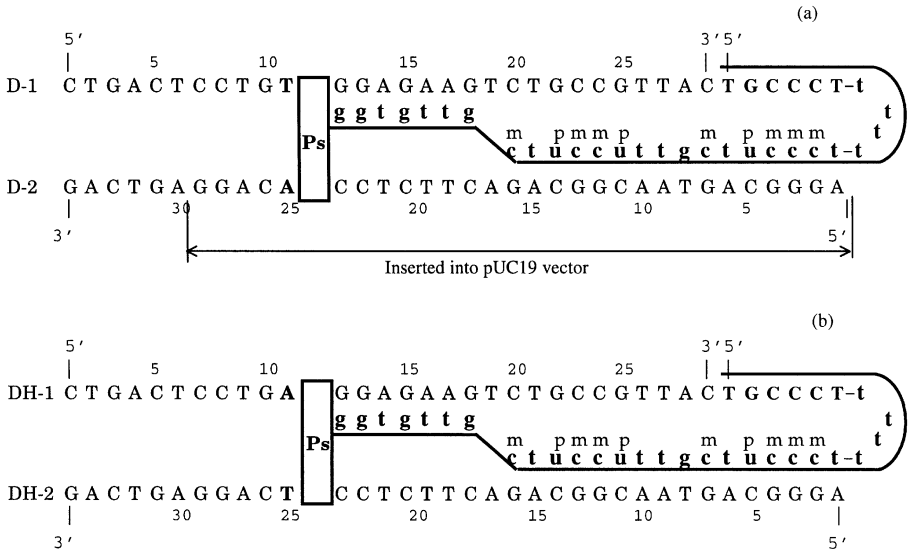

Figure 1. The deoxyoligonucleotide sequence of the β-globin gene fragment that includes the Sickle Cell mutation in codon 6 (**a**) or wild-type sequence (**b**). The mutant T residue and corresponding wild-type A residue are highlighted in bold. The gene target segment inserted into the plasmid is shown in (a). Note the duplex-forming hook at the 5′ end of the third strand, the combination of two third strand-binding motifs that enable strand switching, and the 5-methyl C (mC) and 5-propynyl U (pU) residues in the third strand. The psoralen moiety (Ps) is shown intercalated at the triplex–duplex junction.

gel slices via the 'modified crush-and-soak' method (21). Final purification was by acetonitrile/water (50/50) elution from C18 'Sep-Pak' Reverse Phase columns (Millipore), followed by spin evaporation to dryness. Hydroxymethyltrimethyl psoralen (HMT-psoralen) for the N-4 and N-16 linkers, or aminomethyltrimethyl psoralen (AMT-psoralen) for the N-6 linker (both referred to as psoralen) were attached to the 3′ end of designated oligomers by using psoralen controlled pore glass [CPG; containing a 16 (N-16) or four (N-4) atom linker between HMT-psoralen C-4′ and dimethoxytrityl (DMT) or a six (N-6) atom linker in the case of AMT-psoralen] to initiate oligomer synthesis. (The N-16- and N-4-linked psoralen CPGs were from Chemgene Corp., Waltham, MA, and the CPG with N-6 linker was synthesized at Oncor, Inc.) Linker structures are shown in Figure 2. Oligomer concentrations were adjusted spectrophotometrically in Milli-Q-purified water. Aliquots of purified third strands were analyzed by HPLC to ensure the integrity of attached psoralen. Oligomers were ^{32}P-5′ end-labeled by incubating ~4 pmol of oligomer with 2 μCi of [^{32}P]ATP (Amersham), and 1 U of T-4 polynucleotide kinase (US Biochem) at 37°C for 1 h, purified by denaturing PAGE, and eluted from C18 Sep-Pak columns. The concentration of labeled strands was determined by titration with known amounts of unlabeled complementary strand to form a duplex, which was monitored by quantitative non-denaturing PAGE analysis.

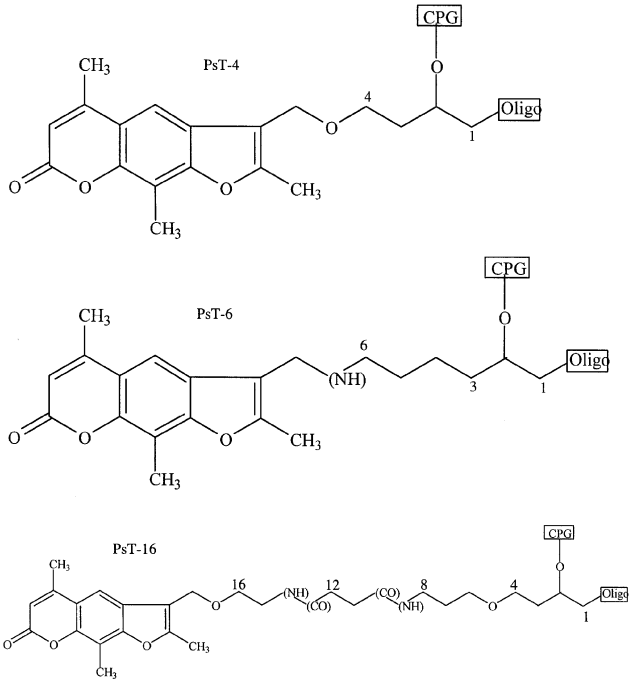

Figure 2. Psoralen–third strand conjugates with varied linker lengths, N.

Duplexes and triplexes

Duplexes were formed by mixing equimolar amounts of each strand, heating to 80°C, and slowly annealing to room temperature in the standard buffer, 0.1 M NaOAc-pH 5.0/ 0.01 M $Mg(OAc)_2$. Various ratios of third strand were added to pre-formed duplex, and the resulting mixtures were incubated for 1 h at room temperature, and then at 4°C overnight to assure maximal formation of triplexes. Unless otherwise noted, duplex concentration was 10 nM and third strand concentration 10-fold higher.

Irradiation conditions

These were as described in the accompanying paper [Broitman *et al.* (22)], using either UVA (365 nm) or visible (419 nm) light, as indicated.

Table 1. Photoproduct distribution on the coding strand (D-1)

Third strand	UVA irradiation (min)	% Total D-1 photoproducts[a]			
		T_{11} MA	T_{11} py-MA[b]	T_9 MA	T_{11} XL
PsT-16	5	55	12	14	19
PsT-16	10	51	11	13	25
PsT-6	5	59	10	15	15
PsT-6	10	54	10	14	22
PsT-4	5	41	12	13	34
PsT-4	10	34	12	12	41

[a]See Materials and Methods for mode of calculation. These values are accurate to within ±2.
[b]py-MA is a pyrone-side psoralen monoadduct.

Table 2. Photoproduct distribution on the non-coding strand (D-2)

Third strand	UVA irradiation (min)	% Total D-2 photoproducts[a]				
		T_{22} MA	C_{23} MA	C_{24} MA	C_{26} MA	XL
PsT-16	5	35	14	16	11	24
PsT-16	10	35	15	16	11	23
PsT-6	5	0	16	28	10	46
PsT-6	10	3	15	26	9	47
PsT-4	5	0	18	7	0	75
PsT-4	10	0	14	6	0	80

[a]See Materials and Methods for mode of calculation. These values are accurate to within ±2.

Electrophoresis

Denaturing PAGE was performed on 25 × 45 cm slabs using 8 M urea/TBE/16% polyacrylamide gels (1:37 bisacrylamide/acrylamide). Samples were dissolved in denaturing loading buffer, 0.005 M EDTA/100% formamide/0.1% bromophenol blue (23), and heated to 80°C before loading. Denaturing gels were run for 2–6 h at 1.5 kV at room temperature. Non-denaturing PAGE was conducted on a 20 × 20 cm slab of 15% polyacrylamide in the standard buffer and run at 4°C for 12 h at 150 V. Denaturing gels were soaked in standard fixing solution (23), then in 100% methanol to remove water (24), and dried on Whatman filter paper on a BioRad gel dryer. Gels were visualized using either or both NEN X-ray film and an ImageQuant PhosphorImager.

Photoproduct quantitation

Labeled photoproduct gel bands were quantitated using an ImageQuant PhosphorImager. Radioactivity measurements of individual bands were corrected for background by subtracting the radioactivity in a same size neighboring part of the gel that was free of a detectable band.

The percentage photoproduct yield for each strand was determined by summing the amounts of radioactivity measured in each photoproduct band and then dividing by the sum of the radioactivity in the unconverted duplex band and that in all the photoproducts, and multiplying by 100.

The distribution of total radioactivity among the different photoproduct bands in any one strand (Tables 1 and 2) or in both strands (Table 3), i.e. the percentage of total photoproducts that any one represents, was calculated as the ratio of radioactivity in each band to the sum of the radioactivity in all the photoproduct bands ×100.

Photoproduct identification by primer extension arrest

Two 8-nt primers, each complementary to the 3′ end of each of the duplex strands, D-1-8, 5′-GTAACGGC-3′; and D-2-8, 5′-CTGACTCC-3′, were synthesized and purified by PAGE. A T7 Sequenase (version 2) DNA sequencing kit (USB) was used for primer extension reactions, with slightly modified reaction conditions. The use of such short primers required lowering the reaction temperature to 14°C and elevating the amount of Sequenase. Duplexes with either the D-1 or D-2 strand labeled were prepared at 10^{-4} M and mixed with third strand, resulting in 5×10^{-5} M duplex and 10^{-4} M third strand in standard buffer. Such a high duplex concentration was required in order to achieve sufficient template (i.e. individual photoproduct of each) concentration in primer extension reactions. After irradiation of triplex mixtures (22), individual photoproducts were separated by denaturing PAGE, cut out, eluted and used as templates in primer extension reactions. Primers were 5′ pre-labeled (23) with [γ-^{32}P]ATP and annealed with templates at 4°C overnight, after which primer extension reactions were performed at 14°C for 4 h.

Third strand binding to plasmid DNA

A plasmid containing the Sickle Cell gene target with the mutant base pair was created by inserting a fragment consisting of the base pairs formed by residues 1–29 of strand D-2 (Fig. 1a) plus a 5′ AATT sticky end and its complement with a 3′ TCGA sticky end into a pUC19 vector between the HindIII and EcoRI sites using DNA ligase (NEB). After purifying with a Qiagen plasmid purification kit, the plasmid was shown by agarose gel electrophoresis to be at least 70% supercoiled.

Table 3. Total photoproduct formation and distribution on the Sickle Cell linear target duplex after 10 min of UVA irradiation

Residue photoproduct	% yield of coding strand[a]			% of total yield on both strands[a]		
	PsT-16	PsT-6	PsT-4	PsT-16	PsT-6	PsT-4
MA $T_{11\ furan}$	18	12	16	36.4	59	28
MA $T_{11\ pyrone}$	6	0.3	5	12.2	1.3	8.7
XL T_{11}	6	0.3	26	12.2	1.3	45.8
MA T_9	4	1	4	8.1	5	7
	% yield of non-coding strand[a]					
T_{22} MA	7	0.1	0	14	0.6	0
C_{23} MA	3	2	4	6	10	7
C_{24} MA	3.5	4	2	7.1	20.2	3.5
C_{26} MA	2	0.5	0	4	2.6	0
XL[b]	5	0.3	27			
Total duplex yield,%	49.5	20.2	57	100	100	100

[a]See Materials and Methods for mode of calculation.
[b]In order not to count crosslink values twice (since each crosslink involves a photoproduct on each strand), only the values for the coding strand are counted to determine the total duplex yield.

Binding to that plasmid of two third strands, PsT-4 (Fig. 2) and PsT-1 (20), was investigated. Mixtures of third strands (10 μM) and plasmid (10 nM) in the standard buffer were incubated at 37°C for 2 h and then overnight at 4°C. After irradiation with UVA light, free third strand was removed, and samples were desalted using Qiagen PCR purification columns. Plasmid–third strand complexes were digested with BanI endonuclease (NEB), and the resulting fragments labeled with ^{32}P and analyzed by native (8%) PAGE.

RESULTS

Kinetics of formation and yield of photoproducts

The structure of the triplex formed between the linear duplex Sickle Cell target and the psoralen-containing third strand is shown in Figure 1a. The psoralen moiety at its 3′ end intercalates into the duplex at various sites permitted by its linker, and upon irradiation can form monoadducts, or cross-links between adjacent pyrimidine residues on opposite strands (22,25,26).

Covalent attachment of the third strand to either one of the duplex strands via psoralen photomodification after irradiation with UVA light results in the appearance of a slower moving triplex band (Fig. 3a) that contains all the photoproducts formed; electrophoretic conditions in TBE buffer do not preserve triplexes with non-covalently bound third strands. All the duplex is not converted to triplex even after long irradiation because not every psoralen moiety intercalated adjacent to a pyrimidine residue forms a photoproduct with that residue (26). Figure 3b shows the time course of total photoproduct formation using third strands with each of the three psoralen linkers. While maximum photoproduct is obtained after ~10 min of UVA irradiation in each case, the yield of photoproduct varies dramatically with the nature of the linker. Almost 85% of the duplex is converted to covalent triplex with PsT-4, ~65% with PsT-16, but only 32% with PsT-6. Yet, electrophoretic analysis of unirradiated triplex mixtures (Fig. 3c) under conditions favorable to triplex stability (standard buffer, 4°C) demonstrates that duplex is quantitatively converted to triplex above 20 nM third strand for PsT-6. HPLC analysis to monitor psoralen integrity revealed no heterogeneity in the third strands with any of the linkers. Taken together, these results show that the lower photoproduct yield with the N-6 third strand is due neither to less triplex formation nor to lower stability or psoralen degradation. Rather, it is probably a consequence of the more rigid structure of its linker, which hinders psoralen photoreaction with nearby pyrimidine residues.

Variation in photoproducts formed by psoralen differently linked to third strands

Such variation was demonstrated in two types of experiments. First, triplexes were formed with radioactively labeled third strands, and products of their covalent attachment to either one (monoadducts) or both (cross-link) duplex strands upon irradiation were analyzed on denaturing PAGE. It was thereby found that the number of different photoproducts is significantly smaller for PsT-6 than for PsT-16, and smaller still for PsT-4 (not shown). Then, to identify and quantitate each of these photoproducts, triplexes with only one or the other duplex strand labeled with ^{32}P (rather than the third strand) were irradiated with UVA light and, after separation by denaturing PAGE, the resulting photoproduct bands (Fig. 4) were cut out, eluted, desalted and used as templates for primer extension analysis.

Primer extension analysis of Sickle Cell target photoproducts

Coding strand D-1. Consistent with our earlier findings (20), third strand-mediated psoralen photoaddition produces two photoproduct bands along this strand. Figure 5 shows a denaturing gel with products of primer extension analysis of the major (Fig. 5a) and the minor (Fig. 5b) monoadducts, as well as a sequencing ladder produced with an unirradiated duplex strand as template. Apparently, Sequenase slows down as the arrest position is approached, and then stops completely, which is why two arrest bands rather than one are observed in Figure 5a. Thus, the farthest 'point of arrest' is identified as the site of psoralen attachment. In the case of strand D-1 with psoralen attached at residue T_9, which could only be isolated in such a small amount that it was difficult to maintain a stable

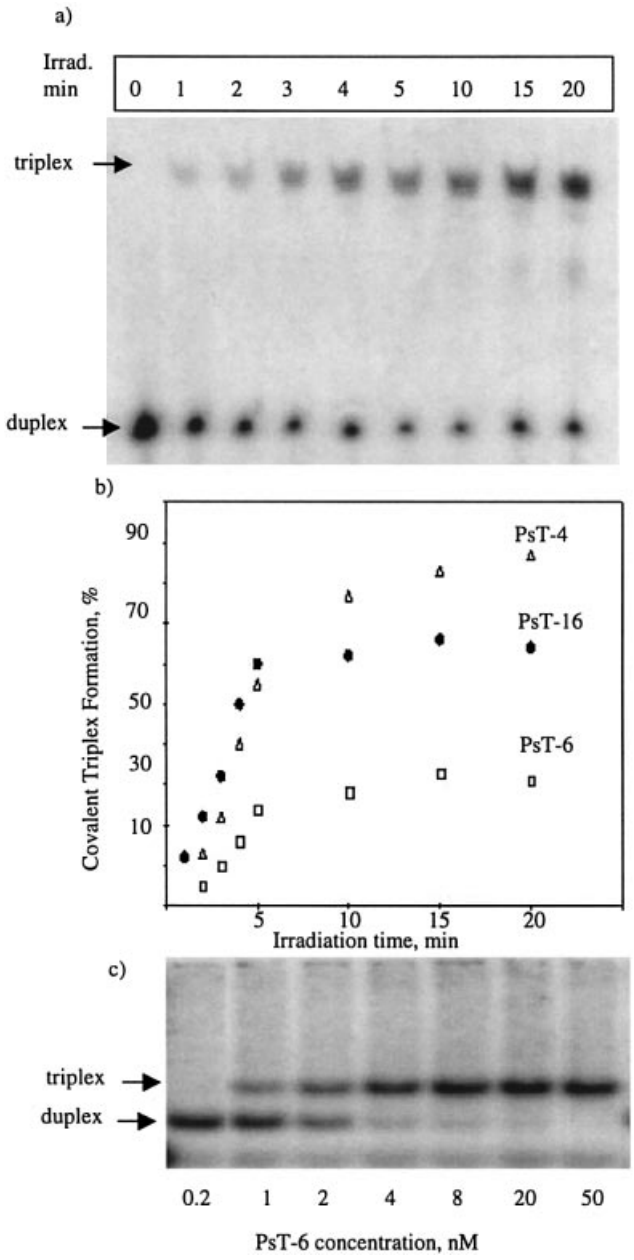

Figure 3. Kinetics of third strand-mediated psoralen photoproduct formation upon UVA irradiation. (**a**) Native PAGE of irradiated triplex mixtures with PsT-16 third strand. Similar gel patterns were obtained with PsT-6 and PsT-4. (**b**) Dependence of covalent triplex formation on UVA irradiation for each third strand. (**c**) PAGE of unirradiated triplexes with increasing PsT-6 third strand concentration in the standard buffer.

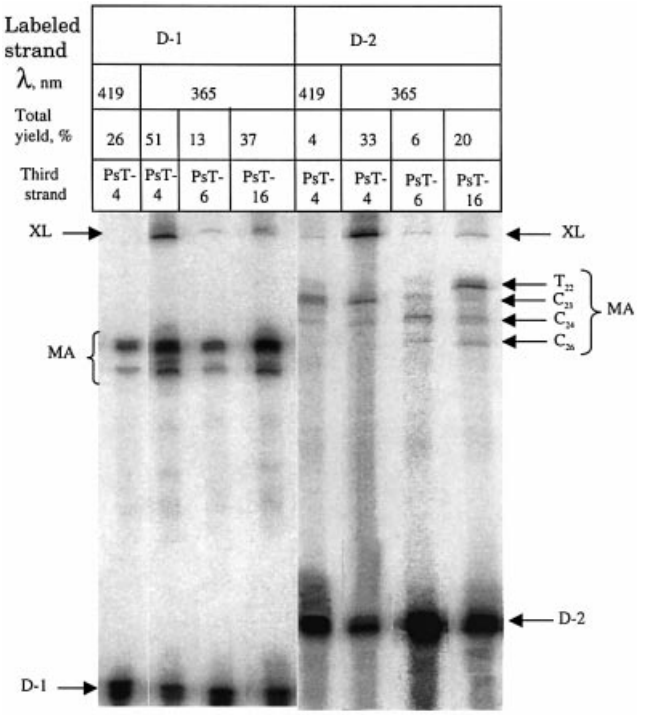

Figure 4. PAGE analysis of photoproducts formed with either target duplex strand and each third strand after irradiation with either 419 (PsT-4) or 365 nm light (Pst-4, PsT-6 and PsT-16).

template–primer duplex, a ladder is observed, rather than just one or two bands, as the point of primer extension arrest is approached (Fig. 5b).

On more slowly run gels that give better resolution, the minor band is seen to consist of two barely distinguishable 'subbands'. One of these is present after irradiation with UVA light but not after irradiation with visible light (Fig. 4, PsT-4 lanes). This indicates that the extra band induced by UV radiation can only be strand D-1 with a pyrone-side monoadduct to either residue T_{11} or T_9 (22). Primer extension analysis (not shown) shows that when this minor monoadduct band, obtained after UV irradiation, is used as a template, the point of arrest does, in fact, correspond to residue T_{11} rather than to residue T_9, as is the case for irradiation with visible light. Only one band is apparent when the monoadduct is at T_9, presumably because the yield of any alternative photoproduct band at this position is too low to be detected.

Table 1 summarizes the distribution of photoproducts between residues T_{11} and T_9 on this strand after irradiation with UVA light. When formation of the faster moving T_{11} pyrone monoadduct D-1 is taken into account, the T_9 residue on the coding strand accounts for 12–14% of total photoproducts regardless of the psoralen linker to the third strand. Apparently, even with the third strand with the shortest linker, residue T_9 remains within easy reach of the psoralen moiety.

Non-coding strand D-2. Denaturing PAGE analysis of strand D-2 labeled photoproducts (Fig. 4) shows that while PsT-16 produces four significant monoadduct bands, PsT-6 produces three and PsT-4 only two in amounts sufficient for further analysis. The reduction in the number of photoproduct bands as the linker is shortened is consistent with intercalation of psoralen at fewer locations. In fact, when used as templates for primer extension arrest (Fig. 6), the monoadduct bands obtained with PsT-16 proved to correspond to psoralen adducts at residues T_{22}, C_{23}, C_{24} and C_{26}, and those with PsT-4 to adducts at residues C_{23} and C_{24}. Table 2 summarizes the distribution of individual photoproducts produced when third strands with the three linkers were used. Note the marked similarity of the values after 5 and 10 min. With PsT-16, the major photoproduct, amounting to 35% of the total photoproducts, is a monoadduct at T_{22}. This could give rise to an

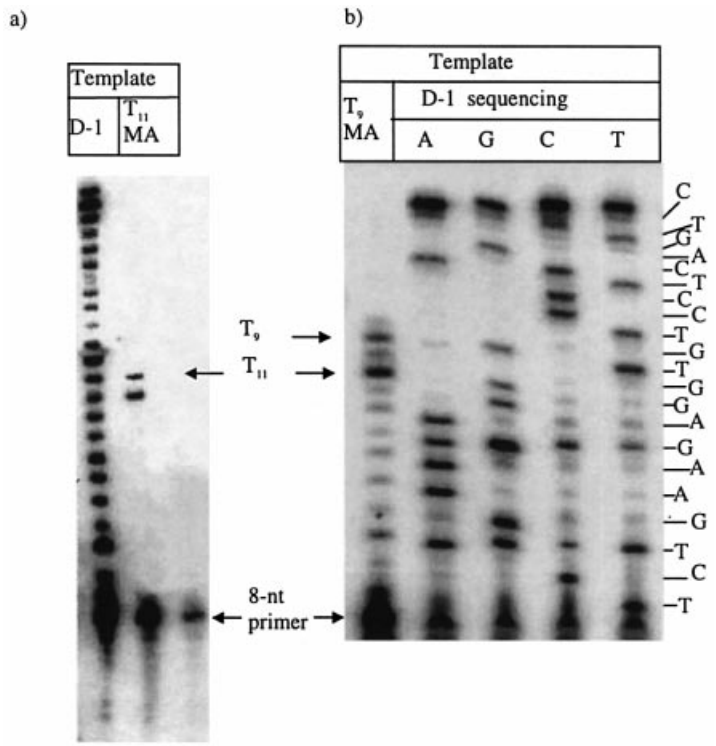

Figure 5. Primer extension analysis of individual photoproducts formed with the D-1 duplex strand. (**a**) The major monoadduct is identified as T_{11}, and (**b**) the minor photoproduct as T_9 (see Fig. 1b).

A→T transversion on the coding strand, resulting in an undesirable glutamate→valine amino acid substitution, comparable with the Sickle Cell mutation itself. Shortening the linker to six atoms (PsT-6) is already sufficient to completely eliminate this undesirable modification. However, it is virtually impossible to avoid photomodification of residues C_{24} and C_{23} using UVA irradiation. C_{24} is the third residue in the antiparallel complement to the mutant GTG codon, and C_{23} is the first in the complement to GAG. Little is known about possible mutagenic consequences of psoralen modification of C residues. To reduce their photomodification, irradiation with visible light could be employed, which also avoids cross-link formation (22). This keeps the same specificity, while drastically reducing the total photoproduct yield for the D-2 strand from 33% after 10 min of irradiation with UVA light to 4% after 4 h with visible light (Fig. 4).

Primer extension analysis of wild-type target photoproducts

As a further application of the primer extension methodology and a test of the specificity of photoproduct formation with the third strand, the interaction of the wild-type target duplex DH-1·DH-2 (in which the $T_{11}{\cdot}A_{25}$ base pair is replaced by $A_{11}{\cdot}T_{25}$) with the PsT-16 and PsT-4 third strands was examined (Fig. 7). After both UVA and visible irradiation, only one DH-1 monoadduct band appears. Both electrophoretic mobility and primer extension arrest show that this monoadduct is formed at the T_9 position (data not shown).

Figure 7 shows similar analysis and identification of photoproducts formed with the non-coding strand DH-2 in which mutant residue A_{25} is replaced by wild-type residue T_{25}. In this case, PsT-4 gives rise to three major photoproducts and a minor one that could not be purified in sufficient amount for primer extension analysis (instead of only two for the D-2 Sickle Cell duplex strand), and PsT-16 to at least four. The monoadduct at residue T_{25} accounts for >50% of total photoproduct on this strand; the minor faster moving monoadduct is most probably a result of alternatively intercalated psoralen interacting with the same T_{25} residue [cf. Broitman *et al*. (22)]. Hence, psoralen photomodification at this site should be exploitable for inducing the Sickle Cell mutation in human cell lines.

Third strand binding to plasmid DNA

As a preliminary to extending this investigation to the cellular level, covalent binding of the psoralen delivery strand to the target in a plasmid (see Materials and Methods) was investigated. In this case, binding was monitored by native PAGE, since mobility of a 299-bp BanI restriction fragment of the plasmid that contains the target is reduced upon covalent (psoralen-mediated) binding of a third strand (Fig. 8), in proportion to the size of that strand. Of the two third strands examined, both with 3′-terminal psoralen, PsT-4 is 33 nt long (Fig. 1), whereas PsT-1 (20) has the 23 nt at the 3′ end of PsT-16, but lacks the binding hook and linker at the 5′ end. The shorter of the third strands, PsT-1, was previously shown to have much lower binding affinity for the linear target than the longer one with the hook (20). The same appears to be true for binding to the plasmid. Whereas 10 μM PsT-4 third strand is sufficient to completely bind to its plasmid targets, PsT-1, which lacks the hook, only binds about half the targets. Thus, the hook facilitates third strand binding to the plasmid, even

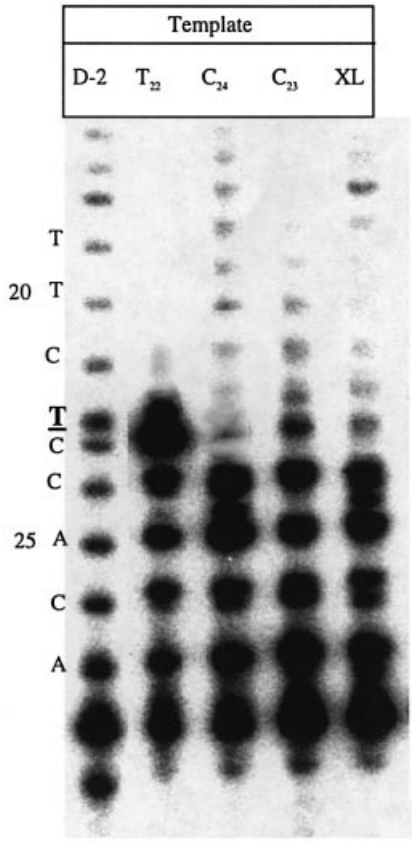

Figure 6. Identification by primer extension arrest of an XL and of monoadducts at T_{22}, C_{23}, C_{24}, C_{26}, each formed with PsT-16 third strand. Lane D-2 shows the ladder obtained with the unmodified D-2 (non-coding) strand.

though the plasmid lacks the complementary sticky end present in the linear target. This effect most probably occurs via strand invasion (27). It is also noteworthy that such strand invasion is more effective with supercoiled plasmids than with relaxed ones (data not shown). In a control experiment with the host plasmid lacking the target, no third strand binding was observed.

DISCUSSION

3′-Terminal positioning of psoralen on the third strand

Because of the target sequence, the third strand required the psoralen moiety to be located at its 3′ end. Hence, specificity of 3′-linked psoralen photomodification at the Sickle Cell mutation site and its dependence on linker length were investigated. By using primer extension arrest to identify individual photoproducts and then phosphorimaging to quantitate and compare their yields, detailed information was obtained about the interaction of such third strand-linked psoralen with its duplex target. This knowledge was then applied to the goal of achieving highly specific psoralen modification of the mutant Sickle Cell residue in the β-globin gene.

Positioning psoralen at the 3′ end of the third strand results in a very different pattern of intercalation than when it is linked to the 5′ end (7,28–30). While 5′-linked psoralen intercalates at the duplex–triplex junction even when there are other pyrimidine residues within reach, 3′-linked psoralen modification is not limited to this site, so that significant interaction with other pyrimidine residues occurs readily. It is also worth noting that C and T residues in the linear target were modified with similar efficiency.

Effects of psoralen linker length

In the present work, the specificity of psoralen photomodification at the Sickle Cell mutation site has been significantly improved by using a shorter psoralen linker. The fraction of the total photoproduct (on D-1 + D-2) represented by the targeted T_{11} residue (furan- and pyrone-side monoadducts and cross-links) is ~60% for PsT-16 and PsT-6, and >80% for PsT-4 (Table 3, Fig. 3). The latter larger fraction of photoproduct at the desired target residue occurs largely because the interaction of psoralen with the non-coding strand is reduced. Undesirable photoaddition to residue T_{22} of the non-coding strand is reduced from 14% of total photoproduct with PsT-16 to undetectable levels with both PsT-6 and PsT-4. This result is important because it essentially eliminates the possibility of a deleterious valine→glutamate substitution at codon 7 that might be phenotypically equivalent to the Sickle Cell valine→glutamate substitution at codon 6. On the other hand, photoaddition to residue T_9 on the coding strand is unaffected by shortening of the linker. This is not surprising since the anticipated span of the N-4 linker (actually six atoms to the psoralen ring × 1.54 Å + psoralen) should encompass a little less than 3 bp (3 × 3.4 Å). It should be noted, however, that none of the base changes possible at this position can influence the amino acid sequence of β-globin, since all possible nucleotide replacements generate codon synonyms. However, they could conceivably impact on message secondary structure and thereby on efficiency of translation. The two C residues on the non-coding strand, C_{24} and C_{23}, are still within reach of the psoralen moiety of the third strand and are therefore susceptible to photomodification. Currently, there is no basis for predicting the mutagenic effects of psoralen photoaddition to these C residues.

It is interesting that there are distinct mobility differences between different monoadducts, even though their molecular weights and net charge must be the same. Their mobility seems to correlate with the distance between the attachment site of the psoralen moiety and the closest end of the duplex strand. This is reasonable, since that distance, in turn, correlates with an ‘overall length’ of the resulting molecule, i.e. the sum of ‘third strand length’ and the distance between the attachment site and the duplex strand end.

The large decrease in the total photoproduct yield when switching from the N-16 to the N-6 linker is surprising. After 20 min of UVA irradiation, the yield of duplex converted to some kind of photoproduct with third strand PsT-16 is 65%, whereas it is only ~30% with PsT-6, and it rises again to nearly 85% for PsT-4 (Fig. 3). A similar trend is also evident after 10 min of UVA irradiation (Table 3). That this reduction with the PsT-6 third strand is not due to a reduction in triplex yield or stability is indicated by the similarity of the binding constants and of bandshift results with the three third strands (not shown). These similarities might be taken to mean that different linker lengths somehow affect the quantum yield of psoralen photoaddition. However, that possibility seems very

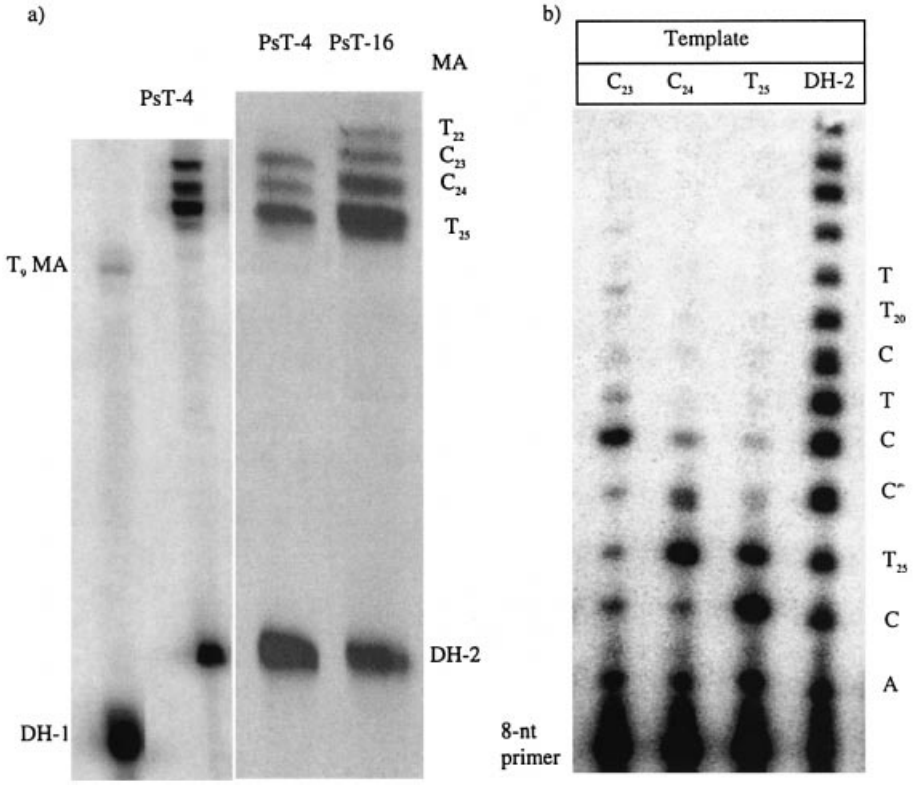

Figure 7. (**a**) Photoproducts formed with the wild-type duplex target sequence DH-1·DH-2 after UVA irradiation and (**b**) their identification by primer extension analysis as monoadducts at C_{23}, C_{24}, T_{25}. Lane DH-2 shows the ladder obtained with the unmodified DH-2 (non-coding strand).

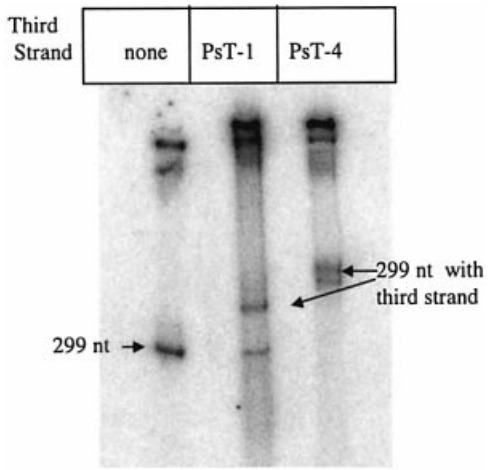

Figure 8. Third strand binding to a plasmid containing the Sickle Cell β-globin target. Covalent attachment of the third strand reduces the mobility of the 299 bp restriction fragment containing the mutation site.

unlikely. More relevant would seem to be the fact that the N-6 linker to AMT-psoralen has an amine linkage in the chain that is likely to make it stiffer and less flexible, which in turn could reduce the efficiency of psoralen intercalation. It is also possible, for example, that the orientation of the intercalated 3′-terminal psoralen is constrained by the shorter and stiffer linker, such that its interaction with a T residue is limited to the unfavorable pyrone side of the psoralen ring, thereby reducing the yield of T photoproducts. In that case, the furan-side monoadducts can only form with C residues on the non-coding strand, which are intrinsically somewhat less reactive (26), resulting in decreased total yield. The increased total yield for the N-4 linker is easier to interpret. Limiting the number of available intercalation sites by shortening the linker inevitably leads to more psoralens intercalated at sites suitable for photomodification; this is especially indicated by the significant increase in cross-link formation with the shortest linker. The cross-link is formed between residue T_{11} on strand D-1 and residue C_{24} on strand D-2 (rather than equally available residue C_{26}), making it a 5′ TpG dinucleotide step, just as 5′ TpA is a preferred site for cross-link formation (26).

The plasmid results reported here are worthy of note. The finding that the third strand with the 'hook' binds more strongly to the plasmid target than the third strand without it demonstrates the added effect of strand invasion on third strand binding.

CONCLUSION

Having studied third strand-mediated photoproduct formation with the linear oligonucleotide model system of the Sickle Cell β-globin gene in great detail, the next step towards evaluating the applicability of our approach to the repair of the Sickle Cell β-globin gene mutation has now been taken. Thus, it has been demonstrated that a third strand with a 3′ psoralen moiety, modified bases and a duplex-forming hook effectively binds as well to the appropriate target within a supercoiled

plasmid. These results, indicating PsT-4 as the third strand with the preferred linker to the photoreactive psoralen moiety, are coupled in the accompanying paper (22) to irradiation conditions that can afford either T_{11} monoadduct or T_{11}-associated crosslink for exploring alternative resultant base changes at the Sickle Cell mutation site induced by DNA repair mechanisms of the human cell.

ACKNOWLEDGEMENTS

We are grateful to Alexander Khorlin for synthesizing a psoralen CPG with the N-6 linker, and to Katherine Lee and Lydia Lin for help with exploratory experiments leading to the present study. This work was supported by NIH grant 1R01 HL63888 from the National Heart, Lung and Blood Institute.

REFERENCES

1. Hobbs,C.A. and Yoon,K.G. (1994) Differential regulation of gene expression *in vivo* by triple helix-forming oligonucleotides as detected by a reporter enzyme. *Res. Dev.*, **4**, 1–8.
2. Kim,H.G., Reddoch,J.F., Mayfield,C., Ebbinghaus,S., Vigneswaran,N., Thomas,S., Jones,D.E. and Miller,D.M. (1998) Inhibition of transcription of the human c-myc protooncogene by intermolecular triplex. *Biochemistry*, **37**, 2299–2304.
3. Giovannangeli,C. and Hélène,C. (1997) Progress in developments of triplex-based strategies. *Antisense Nucleic Acid Drug Des.*, **7**, 413–421.
4. Shen,L.X., Kandimalla,E.R. and Agrawal,S. (1998) Impact of mixed-backbone oligonucleotides on target binding affinity and target cleaving specificity and selectivity by *Escherichia coli* RNase H. *Bioorg. Med. Chem.*, **6**, 1695–1705.
5. Chan,P.P. and Glazer,P.M. (1997) Triplex DNA: fundamentals, advances and potential applications for gene therapy. *J. Mol. Med.*, **75**, 267–282.
6. Wang,G., Levy,D.D., Seidman,M.M. and Glazer,P.M. (1995) Targeted mutagenesis in mammalian cells mediated by intracellular triple helix formation. *Mol. Cell. Biol.*, **15**, 1759–1768.
7. Raha,M., Lacroix,L. and Glazer,P.M. (1998) Mutagenesis mediated by triple helix-forming oligonucleotides conjugated to psoralen: effects of linker arm length and sequence context. *Photochem. Photobiol.*, **67**, 289–294.
8. Fossella,J.A., Kim,Y.J., Shih,H., Richards,E.G. and Fresco,J.R. (1993) Relative specificities in binding of Watson–Crick base pairs by third strand residues in a DNA pyrimidine triplex motif. *Nucleic Acids Res.*, **21**, 4511–4515.
9. Strobel,S.A. and Dervan,P.B. (1992) Triple helix-mediated single-site enzymatic cleavage of megabase genomic DNA. *Methods Enzymol.*, **216**, 309–321.
10. Frank-Kamenetskii,M.D. and Mirkin,S.M. (1995) Triplex DNA structures. *Annu. Rev. Biochem.*, **64**, 65–95.
11. Letai,A.G., Palladino,M., Fromm,E., Rizzo,V. and Fresco,J.R. (1988) Specificity in formation of triple-stranded nucleic acid helical complexes. Studies with agarose-linked polyribonucleotide affinity columns. *Biochemistry*, **27**, 9108–9112.
12. Strobel,S.A., Doucette-Stamm,L.A., Riba,L., Houseman,D.E. and Dervan,P.B. (1991) Site-specific cleavage of human chromosome 4 mediated by triple-helix formation. *Science*, **254**, 1639–1642.
13. Vasquez,K.M., Dagle,J.M., Weeks,D.L. and Glazer,P.M. (2001) Chromosome targeting at short polypurine sites by cationic triplex-forming oligonucleotides. *J. Biol. Chem.*, **276**, 38536–38541.
14. Giovannangeli,C., Diviacco,S., Labrousse,V., Gryaznov,S., Charneau,P. and Hélène,C. (1997) Accessibility of nuclear DNA to triplex-forming oligonucleotides: the integrated HIV-1 provirus as a target. *Proc. Natl Acad. Sci. USA*, **94**, 79–84.
15. Vasquez,K.M., Wang,G., Havre,P.A. and Glazer,P.M. (1999) Chromosomal mutations induced by triplex-forming oligonucleotides in mammalian cells. *Nucleic Acids Res.*, **27**, 1176–1181.
16. Reardon,J.T., Spielmann,P., Huang,J.C., Sastry,S., Sancar,A. and Hearst,J.R. (1991) Removal of psoralen monoadducts and crosslinks by human cell free extracts. *Nucleic Acids Res.*, **19**, 4623–4629.
17. Duval-Valentin,G., Takasugi,M., Hélène,C. and Sage,E. (1998) Triple helix-directed psoralen crosslinks are recognized by Uvr(A)BC excinuclease. *J. Mol. Biol.*, **278**, 815–825.
18. Majumdar,A., Puri,N., Cuenoud,B., Natt,F., Martin,P., Khorlin,A., Dyatkina,N., George,A.J., Miller,P.S. and Seidman,M.M. (2003) Cell cycle modulation of gene targeting by a triple helix-forming oligonucleotide. *J. Biol. Chem.*, **278**, 11072–11077.
19. Wang,G. and Glazer,P.M. (1995) Altered repair of targeted psoralen photoadducts in the context of an oligonucleotide-mediated triple helix. *J. Biol. Chem.*, **270**, 22595–22601.
20. Broitman,S., Amosova,O., Dolinnaya,N. and Fresco,J.R. (1999) Repairing the Sickle Cell mutation. I. Specific covalent binding of a photoreactive third strand to the mutated base pair. *J. Biol. Chem.*, **274**, 21763–21768.
21. Chen,Z. and Ruffner,D.E. (1996) Modified crush-and-soak method for recovering oligodeoxynucleotides from polyacrylamide gel. *Biotechniques*, **21**, 820–822.
22. Broitman,S.L., Amosova,O. and Fresco,J.R. (2003) Repairing the Sickle Cell mutation. III. Effect of irradiation wavelength on the specificity and type of photoproduct formed by a 3′-terminal psoralen on a third strand directed to the mutant base pair. *Nucleic Acids Res.*, **31**, 4682–4688.
23. Maniatis,T. Fritsch,E.F. and Sambrook,J. (1982) *Molecular Cloning: A Laboratory Manual*. Cold Spring Harbor Laboratory Press, Cold Spring Harbor, NY.
24. Thomas,M., Abedi,H. and Farzaneh,F. (1992) Procedure for drying high-percentage acrylamide gels. *Biotechniques*, **13**, 533.
25. Sage,E. and Moustacchi,E. (1987) Sequence context effects on 8-methoxypsoralen photobinding to defined DNA fragments. *Biochemistry*, **26**, 3307–3314.
26. Hearst,J.E., Isaacs,S.T., Kanne,D., Rapoport,H. and Straub,K. (1984) The reaction of the psoralens with deoxyribonucleic acid. *Q. Rev. Biophys.*, **17**, 1–44.
27. Gamper,H.B.,Jr, Hou Y.-M., Stamm,M.R., Podyminogin,M.A. and Meyer,R.B. (1998) Strand invasion of supercoiled DNA by oligonucleotides with a triplex guide sequence. *J. Am. Chem. Soc.*, **120**, 2182–2183
28. Oh,D.H. and Hanawalt,P.C. (2000) Binding and photoreactivity of psoralen linked to triple helix-forming oligonucleotides. *Photochem. Photobiol.*, **72**, 298–307.
29. Perkins,B.D., Wensel,T.G., Vasquez,K.M. and Wilson,J.H. (1999) Psoralen photo-cross-linking by triplex-forming oligonucleotides at multiple sites in the human rhodopsin gene. *Biochemistry*, **38**, 12850–12859.
30. Bates,P.J., Macaulay,V.M., McLean,N.J., Jenkins,T.C., Reszka,A.P., Laughton,C.A. and Niedle,S. (1995) Characteristics of triplex-directed photoadduct formation by psoralen-linked oligodeoxynucleotides. *Nucleic Acids Res.*, **23**, 4283–4289.